

Experimental and theoretical density-dependent absorption spectra in (GaInSb/InAs)/AlGaSb superlattice multiple quantum wells

J. T. Olesberg,^{a)} S. A. Anson,^{b)} S. W. McCahon,^{c)} Michael E. Flatté,^{d)} and Thomas F. Boggess^{e)}

Department of Physics and Astronomy, Optical Science and Technology Center, University of Iowa, Iowa City, Iowa 52242

D. H. Chow and T. C. Hasenberg^{f)}
Hughes Research Laboratories, Malibu, California 90265

(Received 30 July 1997; accepted for publication 8 November 1997)

A broadly tunable, ultrafast optical parametric oscillator is used to measure carrier-density-dependent absorption spectra in a 340-meV band gap (GaInSb/InAs)/AlGaSb superlattice multiple quantum well structure. Similar structures have been implemented recently as the active region in midinfrared diode lasers. The measured spectra are compared with calculated spectra computed using a semiempirical eight-band superlattice $\mathbf{K}\cdot\mathbf{p}$ model. The model provides good agreement with the experimentally observed spectral and density dependence of the absorption. These results provide confirmation that the model may be used for band structure engineering of optimized midinfrared laser active regions. © 1998 American Institute of Physics. [S0003-6951(98)02102-0]

The development of efficient, high-power semiconductor lasers operating in the 2–5 μm spectral region (midwave infrared)^{1–6} is of interest for applications that include remote sensing, infrared imaging systems, infrared countermeasures, and medical diagnostics. Future advances in the design, growth, and fabrication of these lasers will be closely tied to advances in the ability to model the optical and electronic properties of the heterostructures from which they are comprised. Advances in modeling follow three iterative steps: (1) the development of accurate band structure models, (2) application of these models to calculations of optical and electronic properties, and (3) testing of these theoretical predictions through comparison with experimental data. Models that have been calibrated in such a manner may then be applied to the optimization of device design through band structure engineering. This letter serves as a verification of the model that we have used in the design of midwave infrared heterostructure active regions.⁷

Carrier density-dependent absorption (or gain) spectra, along with carrier lifetimes, are essential material properties for diode laser performance. The accuracy of calculated absorption spectra depend on both the accuracy of the computed band structure and the model used for the density dependence of the absorption. If the results are to be used to optimize device performance, it is crucial that such computed quantities be verified through comparison with measured results. Here, we directly measure the density-dependent absorption spectra using time-resolved differential transmission with a broadly tunable, midinfrared, optical

parametric oscillator⁸ and compare the results with a band-filling model for the absorption based on a $\mathbf{K}\cdot\mathbf{p}$ calculation of the band structure.⁹ We find that the measured and calculated spectra are in good agreement over a wide range of carrier densities including those expected during diode laser operation, and over a wide spectral range that includes contributions from higher conduction subbands. These results indicate that the calculated band structure, together with the band filling model, are sufficiently accurate to provide the basis for optimizing these structures for diode laser active regions.

The structure under investigation was grown by molecular beam epitaxy on an undoped GaSb substrate and contains ten 225 Å quantum wells separated by 400 Å $\text{Al}_{0.2}\text{Ga}_{0.8}\text{Sb}$ barriers. Each well [shown in Fig. 1(a)] is composed of a short segment of a type II (misaligned) GaInSb/InAs superlattice consisting of five 33 Å $\text{Ga}_{0.75}\text{In}_{0.25}\text{Sb}$ layers and four

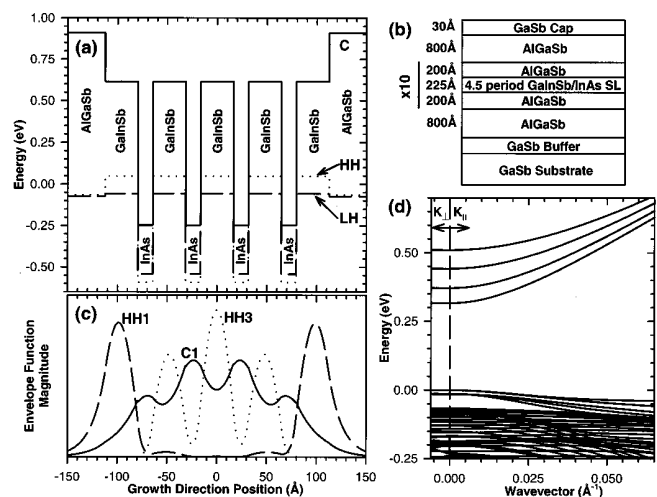


FIG. 1. (a) Band-edge diagram of one superlattice quantum well, (b) schematic of the epitaxial structure, (c) magnitude of the envelope functions for states near the band edge, and (d) band structure in the growth direction (K_{\perp}) and parallel to the interfaces (K_{\parallel}).

^{a)}Electronic mail: jonathon-olesberg@uiowa.edu

^{b)}Department of Electrical and Computer Engineering, University of Iowa, Iowa City, Iowa 52242.

^{c)}Hughes Missile Systems Group, Tucson, Arizona.

^{d)}Electronic mail: flatte@rashi.physics.uiowa.edu

^{e)}Also with the Department of Electrical and Computer Engineering, University of Iowa. Electronic mail: thomas-boggess@uiowa.edu

^{f)}Present address: Department of Physics and Astronomy, Optical Science and Technology Center, University of Iowa, Iowa City, Iowa 52242.

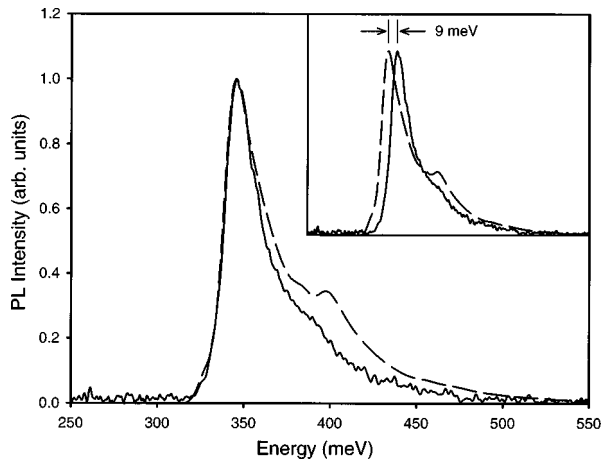


FIG. 2. Measured (solid line) and calculated (dashed line) room temperature photoluminescence. For a better indication of the agreement, the calculation has been shifted 9 meV so that the low-energy peaks are at the same energy. The inset shows the curves before the shift.

15 Å InAs layers. Similar structures have been used successfully as the active region in 3–4 μm diode lasers.¹ A schematic of the epitaxial structure of the nominally undoped sample is shown in Fig. 1(b).

The optical properties of the sample have been calculated using the full nonparabolic band structure obtained from a superlattice $\mathbf{K}\cdot\mathbf{p}$ model based on eight bulk bands.⁹ A phenomenological heavy-hole mass is used to incorporate the effects of more remote bands. Absorption spectra calculations make use of momentum-dependent optical matrix elements and include intersubband absorption. The calculation described in Ref. 9 has been extended so that the periodic unit cell consists of the short (4.5 period) GaInSb/InAs superlattice well and the AlGaSb barrier. In this way, edge effects of the short superlattice well are included. The input parameters¹⁰ to the $\mathbf{K}\cdot\mathbf{p}$ calculation, which include the band gap, spin-orbit splitting, heavy-hole mass, and band offsets of the constituent layers, are tabulated in Ref. 9. Strain effects are included through the use of deformation potentials.

The calculated envelope functions for some of the band-edge states are shown in Fig. 1(c) and the band structure is shown in Fig. 1(d). The HH1 state is localized near the edge of the quantum well due to the small AlGaSb/GaInSb valence band offset compared with the InAs/GaInSb offset. The small overlap between C1 and HH1 results in a small matrix element (1/3 that of the C1–HH3 matrix element).¹¹ The top five hole levels (one heavy-hole state for each GaInSb layer) are nearly degenerate while the four lowest conduction band levels are spaced approximately equally 60 meV apart. The C1 mass is $0.029m_0$ (where m_0 is the free electron mass). The small C1–HH1 matrix element and the multiplicity of band-edge valence subbands have a negative impact on laser performance in related laser structures.⁷

The 300 K photoluminescence (PL) from the sample under cw near-infrared diode laser excitation is shown in Fig. 2. These measurements give a reasonable estimation of the band-gap energy and the quality of the sample. The room-temperature PL, which is strong and peaked near 345 meV, agrees well with the calculated PL. The excitation density for the calculated PL is 10^{15} cm^{-3} , which is the density esti-

ated for the cw PL measurements using the excitation intensity and Shockley–Read–Hall lifetime. In this and subsequent figures, the displayed calculations include 10 meV of broadening using a Gaussian line shape which approximates the effect of monolayer layer thickness fluctuations. The 9 meV difference (3% of the band gap) between the peaks of the calculated and measured PL spectra is within the uncertainty in the calculated band gap due to uncertainties in the input parameters, such as the difference between the nominal and actual layer thicknesses in the grown structure. The low-energy peak is associated primarily with the C1–HH3 transition, while the shoulder near 390 meV is due to the C2–HH4 transition.

In principle, detailed information about the electronic structure in the sample can be obtained from a calibrated linear transmission spectrum. Unfortunately, the small band edge absorption coefficient ($\sim 2000\text{ cm}^{-1}$) and the short length ($0.225\text{ }\mu\text{m}$) of active material in the structure result in weak absorption (approximately 4% at the band edge). This weak absorption is superposed on a strong, spectrally varying, background absorption associated with free-carrier transitions in the undoped but nominally p -type GaSb substrate. Correction for the substrate absorption is difficult as a consequence of variations in background impurity concentrations among substrates as well as inhomogeneities within a given substrate. In contrast, PL and differential transmission measurements are unaffected by the substrate absorption spectrum.

Measurements of density-dependent transmission¹² were performed using 140 fs pump pulses from a mode-locked Ti:sapphire laser operating between 1.48 and 1.55 eV and 170 fs probe pulses from a synchronously pumped optical parametric oscillator with photon energies between 320 and 470 meV. An improvement over the work in Ref. 12 is the addition of a monochromator to increase the spectral resolution to approximately 5 meV, while preserving the temporal resolution of the measurement. The differential probe transmission, $\Delta T/T_0$, was related to the change in absorption, $\Delta\alpha$, using $\Delta\alpha = \ln(\Delta T/T_0 + 1)/L$, where L , is the width of the absorbing region ($0.225\text{ }\mu\text{m}$). Measurements of $\Delta\alpha$ were conducted as a function of probe energy and pump power.

Given the large excess energy with which the carriers are injected (over 1 eV), we expect that some carriers will be lost in the substrate beyond the active region, and we assume that the rest will be evenly distributed among the ten wells. We account for the loss of carriers using a single capture efficiency, which is defined as the fraction of injected carriers which remain in the active region. Most carriers are trapped in the wells, where they cool and ultimately fill states near the band edge. The differential transmission peaks approximately 20 ps after excitation, at which point the capture and cooling processes are effectively complete.

At low densities, no significant recombination occurs in the time that it takes for the carriers to cool to the band edge. At the highest densities in this study, Auger recombination reduces the carrier lifetime to less than 75 ps. We account for carriers that recombine before they cool to the band edge using previously measured density-dependent recombination rates.¹²

The measured $\Delta\alpha$ spectra are shown in Fig. 3(a) for

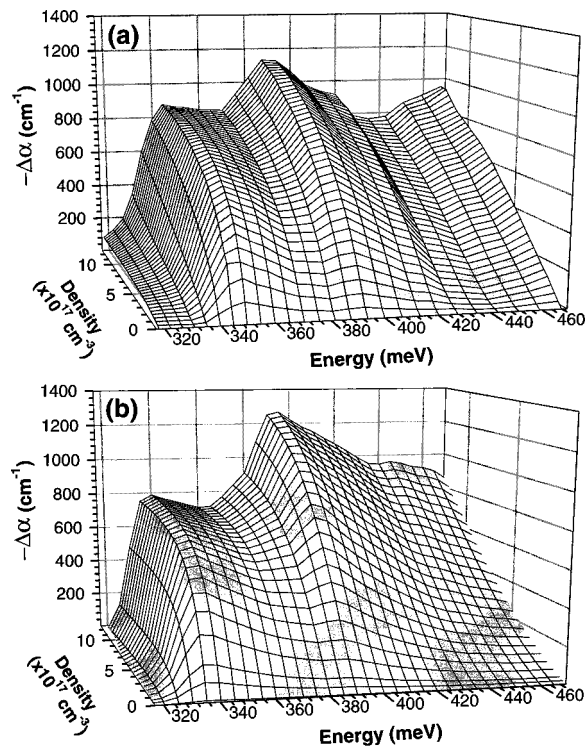


FIG. 3. (a) Measured and (b) calculated change in absorption ($\Delta\alpha$) as a function of density and energy. For easier visualization, $-\Delta\alpha$ is shown.

densities from 0.5×10^{17} to $12.0 \times 10^{17} \text{ cm}^{-3}$. The density axis is obtained using a capture efficiency of 73%, which provides the best agreement with the calculated spectra, shown in Fig. 3(b). $\Delta\alpha$ is nonzero over a wide spectral range, and has a steplike behavior characteristic of quasi-two-dimensional systems. We associate the lowest energy peak near 340 meV with blocking of transitions to the first conduction subband (primarily C1–HH3) and the higher energy peak near 390 meV with blocking of transitions to the second conduction subband (primarily C2–HH4). The spectral positions of these features are consistent with the peak and shoulder seen in the PL spectrum. Small shoulders in the absorption at 320 meV (obscured by intersubband absorption) and 375 meV are due to the weak C1–HH1 and C2–HH2 transitions, respectively.

Overall, the agreement between theory and experiment is excellent, and even compares favorably with the agreement obtained in bulk GaAs.¹³ We emphasize that the capture efficiency is the only variable parameter used to optimize the agreement between the calculation and measurement. The calculated change in absorption from the band edge through the C2–HH4 transition at 390 meV is within 25% of the experimental value for all densities. The underestimation of the change in absorption at low energies is due in part to the neglect of bleaching of the Sommerfeld enhancement factor in our calculations. Calculations of the Sommerfeld enhancement factor for GaInAs/AlInAs superlattices suggest that it is approximately 20% of the bare absorption.¹⁴ Band-gap renormalization and density-dependent broadening are suggested by the data but are small (renormalization is on the order of the resolution of our measurements: ~ 10 meV). The overestimation of the change in absorption for the C2–HH4

transition is consistent with the overestimation of the shoulder in the calculated PL spectra observed at 400 meV in Fig. 2.

The main discrepancy between the calculation and the measurements occurs at the highest energies (more than 100 meV above the band edge), where the data show an increase, suggestive of the blocking of states in the third conduction subband. It should be noted that the theory does predict a rise at these energies for slightly higher densities (not shown). The delay in bleaching may be caused by an overestimation of the calculated density of states between and the band edge and this transition, which results in an underestimation of the electron density in the third conduction subband (bleaching is dominated by occupation of the conduction band states for all densities considered due to the large heavy-hole mass and the degeneracy of the top five valence states).

In summary, we have performed measurements of density-dependent absorption spectra in a superlattice multiple quantum well. These measurements are in good agreement over a wide spectral range with spectra calculated using a superlattice $\mathbf{K}\cdot\mathbf{p}$ model. These results indicate that the model is sufficiently accurate to provide the basis for optimizing these structures for diode laser active regions.

This research was supported in part by the U.S. Air Force, Air Force Material Command, Phillips Laboratory (PL), Kirtland AFB, NM 87117-5777 (Contract No. F29601-97-C0041) and the National Science Foundation (Grant Nos. ECS-9406680 and ECS-9707799).

¹T. C. Hasenberg, R. H. Miles, A. R. Kost, and L. West, IEEE J. Quantum Electron. **33**, 1403 (1997); T. C. Hasenberg, D. H. Chow, A. R. Kost, R. H. Miles, and L. West, Electron. Lett. **31**, 275 (1995).

²H. K. Choi, G. W. Turner, M. J. Manfra, and M. K. Connors, Appl. Phys. Lett. **68**, 2936 (1996).

³J. I. Malin, C. L. Felix, J. R. Meyer, C. A. Hoffman, J. F. Pinto, C.-H. Lin, P. C. Chang, S. J. Murry, and S.-S. Pei, Electron. Lett. **32**, 1593 (1996).

⁴S. R. Kurtz, R. M. Biefeld, A. A. Allerman, A. J. Howard, M. H. Crawford, and M. W. Pelczynski, Appl. Phys. Lett. **68**, 1332 (1996).

⁵D. Z. Garbuzov, R. U. Martinelli, H. Lee, R. J. Menna, P. K. York, L. A. DiMarco, M. G. Harvey, R. J. Matarese, S. Y. Narayan, and J. C. Conolly, Appl. Phys. Lett. **70**, 2931 (1997).

⁶J. Faist, F. Capasso, C. Sirtori, D. L. Sivco, J. N. Baillargeon, A. L. Hutchinson, S.-N. G. Chu, and A. Y. Cho, Appl. Phys. Lett. **68**, 3680 (1996).

⁷M. E. Flatté, J. T. Olesberg, S. A. Anson, T. F. Boggess, T. C. Hasenberg, R. H. Miles, and C. H. Grein, Appl. Phys. Lett. **70**, 3212 (1997).

⁸S. W. McCahon, S. A. Anson, D.-J. Jang, and T. F. Boggess, Opt. Lett. **20**, 2309 (1995).

⁹M. E. Flatté, C. H. Grein, H. Ehrenreich, R. H. Miles, and H. Cruz, J. Appl. Phys. **78**, 4552 (1995); M. E. Flatté, P. M. Young, L.-H. Peng, and H. Ehrenreich, Phys. Rev. B **53**, 1963 (1996).

¹⁰See, *Semiconductors: Group IV Elements and III–V Compounds*, edited by O. Madelung (Springer, New York, 1991).

¹¹M. E. Flatté, C. H. Grein, J. T. Olesberg, and T. F. Boggess, Mater. Res. Soc. Symp. Proc. **450**, 85 (1997).

¹²S. W. McCahon, S. A. Anson, D.-J. Jang, M. E. Flatté, T. F. Boggess, D. H. Chow, T. C. Hasenberg, and C. H. Grein, Appl. Phys. Lett. **68**, 2135 (1996).

¹³Y. H. Lee, A. Chavez-Pirson, S. W. Koch, H. M. Gibbs, S. H. Park, J. Morhange, A. Jeffery, and N. Peyghambarian, Phys. Rev. Lett. **57**, 2446 (1986).

¹⁴P. M. Young, P. M. Hui, and H. Ehrenreich, Phys. Rev. B **44**, 12969 (1991).